

Characterizing unforced multi-decadal variability of ENSO: a case study with the GFDL CM2.1 coupled GCM

A. R. Atwood^{1,2}  · D. S. Battisti³ · A. T. Wittenberg⁴ · W. H. G. Roberts⁵ · D. J. Vimont⁶

Received: 29 March 2016 / Accepted: 29 November 2016 / Published online: 26 December 2016
© Springer-Verlag Berlin Heidelberg 2016

Abstract Large multi-decadal fluctuations of El Niño–Southern Oscillation (ENSO) variability simulated in a 4000-year pre-industrial control run of GFDL CM2.1 have received considerable attention due to implications for constraining the causes of past and future changes in ENSO. We evaluated the mechanisms of this low-frequency ENSO modulation through analysis of the extreme epochs of CM2.1 as well as through the use of a linearized intermediate-complexity model of the tropical Pacific, which produces reasonable emulations of observed ENSO variability. We demonstrate that the low-frequency ENSO modulation can be represented by the simplest model of a linear, stationary process, even in the highly nonlinear CM2.1. These results indicate that CM2.1’s ENSO modulation is driven by transient processes that operate at interannual or shorter time scales. Nonlinearities and/or multiplicative

noise in CM2.1 likely exaggerate the ENSO modulation by contributing to the overly active ENSO variability. In contrast, simulations with the linear model suggest that intrinsically-generated tropical Pacific decadal mean state changes do not contribute to the extreme-ENSO epochs in CM2.1. Rather, these decadal mean state changes actually serve to *damp* the intrinsically-generated ENSO modulation, primarily by stabilizing the ENSO mode during strong-ENSO epochs. Like most coupled General Circulation Models, CM2.1 suffers from large biases in its ENSO simulation, including ENSO variance that is nearly twice that seen in the last 50 years of observations. We find that CM2.1’s overly strong ENSO variance directly contributes to its strong multi-decadal modulation through broadening the distribution of epochal variance, which increases like the square of the long-term variance. These results suggest that the true spectrum of unforced ENSO modulation is likely substantially narrower than that in CM2.1. However, relative changes in ENSO modulation are similar between CM2.1, the linear model tuned to CM2.1, and the linear model tuned to observations, underscoring previous findings that relative changes in ENSO variance can robustly be compared across models and observations.

Electronic supplementary material The online version of this article (doi:10.1007/s00382-016-3477-9) contains supplementary material, which is available to authorized users.

✉ A. R. Atwood
aatwood@berkeley.edu

¹ Geography Department, UC Berkeley, Berkeley, CA 94709, USA

² Department of Earth and Atmospheric Sciences, Georgia Institute of Technology, Atlanta, GA 30332, USA

³ Department of Atmospheric Sciences, University of Washington, Seattle, WA 98195, USA

⁴ NOAA Geophysical Fluid Dynamics Laboratory, Princeton, NJ, USA

⁵ School of Geographical Sciences, University of Bristol, Bristol BS8 1SS, UK

⁶ Atmospheric and Oceanic Sciences Department, University of Wisconsin-Madison, Madison, WI 53705, USA

Keywords ENSO · Multi-decadal variability · GFDL CM2.1 · Linearized model · Nonlinear feedbacks

1 Introduction

The decadal- and longer-scale modulation of ENSO is a critical element of past and future climate variations, yet it is poorly constrained by the short observational record (Capotondi et al. 2015; Wittenberg 2015). ENSO variability is thought to have exhibited large changes over

the Holocene (Cobb et al. 2013; Koutavas et al. 2006; McGregor et al. 2013; Tudhope et al. 2001), however it is not yet known to what extent these variations are forced, versus inherent to a noisy coupled ocean–atmosphere system. This uncertainty arises in part from poor observational constraints on the unforced intrinsic component of ENSO modulation on multi-decadal and longer timescales.

Given the short observational record of tropical Pacific climate variability, long unforced simulations of the climate system with fully coupled General Circulation Models (GCMs) are helpful for investigating ENSO variability on decadal and longer timescales (Russon et al. 2014; Wittenberg 2009). A 4000 year-long pre-industrial control run of GFDL CM2.1 (Delworth et al. 2006; Wittenberg et al. 2006) has been shown to exhibit strong, unforced, largely unpredictable, multi-decadal changes in ENSO variability (Karamperidou et al. 2014; Kug et al. 2010; Wittenberg 2009; Wittenberg et al. 2014), which also influence the background climatological state of the tropical Pacific (Ogata et al. 2013). These large low-frequency ENSO modulations suggest that in order to detect a forced change in ENSO variability (e.g. from paleoclimate proxies or observations), long records are needed.

However, large ENSO biases prevalent in GCMs obscure the real-world relevance of the tropical climate variability obtained from GCM simulations (Guilyardi 2016). GCMs used in the Fourth and Fifth Assessment Reports of the Intergovernmental Panel on Climate Change exhibit a wide range of biases in their representation of ENSO variability, including biases in the amplitude of variance, spatial pattern of SST variability, distribution of ENSO SST anomalies, and seasonal synchronization of ENSO (An and Wang 2000; Bellenger et al. 2014; Capotondi et al. 2015; Graham et al. 2016; Guilyardi et al. 2009, 2012a, b), which has resulted in little agreement on how ENSO is likely to change in the future (Cai et al. 2014; Chen et al. 2016; Collins et al. 2010; DiNezio et al. 2012; Taschetto et al. 2014; Watanabe et al. 2012). The sources of these ENSO biases are largely unknown, but likely result partly from mean state biases in the models. In this study, we investigate the sources of the low-frequency ENSO modulation by performing further analyses of ENSO in the CM2.1 control run, observations, and that simulated by a linearized intermediate model of the tropical Pacific. Through this process, we evaluate the influence of the overly active interannual variability in CM2.1 on the interdecadal modulation of ENSO in an effort to improve constraints on the true spectral characteristics of ENSO in nature.

Because the CM2.1 control simulation is unforced, there are essentially four, non mutually exclusive, mechanisms that could cause the large multi-decadal ENSO variability: (1) low frequency changes in the tropical Pacific mean state, which alter the stability of the ENSO system; (2)

low frequency changes in stochastic (weather) processes that influence ENSO; (3) random sampling from a stationary, linear process; and (4) nonlinear dynamics, including multiplicative noise, in the ENSO system that spreads variance over a range of time scales. Using the linear model, we show that linear dynamics acting in response to low frequency changes in the tropical Pacific mean state are not the source of low-frequency ENSO modulation in CM2.1. While the influence of low frequency changes in stochastic noise is difficult to address using the suite of tools employed in this analysis, we demonstrate using the linear model runs, CM2.1, and observations that random variations associated with a stationary, linear process are important. Our analyses lead us to conclude that the nonlinearities are also inextricably linked to the multi-decadal ENSO modulation in CM2.1, and while they do not dramatically broaden the distribution of variance as compared to a linear system with equal (i.e. overly active) ENSO variability, they likely shape the distribution of absolute ENSO modulation by contributing to the overly active ENSO variability.

2 Description of the linearized model

The Linearized Ocean Atmosphere Model (LOAM; Thompson and Battisti 2000) is a linearized variant of the (Zebiak and Cane 1987) intermediate complexity model of the tropical Pacific, updated to include observationally constrained parameter values and observed climatological mean state fields, including ocean currents and vertical thermal structure (Thompson 1998a, b; Roberts 2007). LOAM is constructed as an anomaly model, such that it calculates the anomalies of its state variables about a set of prescribed mean states. These mean state variables determine the details of the behavior of ENSO in the model. Because the mean states are explicitly prescribed in the model, it is an ideal tool to investigate how changes in these mean states can alter the behavior of ENSO. Indeed it has been shown (Roberts and Battisti 2011; Roberts et al. 2014) that relatively small changes in the mean states can result in relatively large changes in the behavior of ENSO. The set of seasonally varying mean fields required by LOAM are the SST, near-surface winds, vertical structure of ocean temperature along the equator, upper ocean currents and upwelling. To understand what can cause a change in the behavior of ENSO between two climate states it is possible to use individual mean states from either climate to isolate, for example, the impact of changing the mean wind. The governing equations in LOAM are provided in the Supplementary material (S.1), along with a summary of the constants and tuning parameters used in LOAM (Table S1; Fig. S1).

Briefly, LOAM is comprised of a 1.5-layer ocean model and a two-layer atmosphere model in which heating is a function of SST and surface wind convergence (Gill 1980). The atmosphere is linear, and modeled as a single baroclinic mode on an equatorial β -plane, with mechanical and thermodynamic damping. In contrast to the Zebiak and Cane (1987) model and the Battisti (1988) model, the atmospheric convergence feedback has been linearized as in Battisti and Hirst (1989). The ocean model consists of an active upper layer, governed by the linear shallow water equations on an equatorial β -plane, and a motionless lower layer. A 50 m deep Ekman layer, assumed to be in steady state with the surface winds, is embedded in the active upper layer. The linearized prognostic equation for sea surface temperature (SST) includes three-dimensional advection of temperature anomalies by the climatological currents, anomalous advection of the climatological temperature, vertical mixing, and a simple parameterization of the surface heat flux (Roberts and Battisti 2011; Thompson 1998b). The dependent variables for the ocean are: meridional and zonal current, thermocline depth, and SST perturbations. The ocean equations are spectrally discretized in the meridional direction by projecting them onto Rossby wave space, and discretized in the zonal direction using finite differences. The atmosphere and SST equations are projected onto Hermite functions in the meridional direction, and are discretized in the zonal direction using finite differences.

There are three parameters in LOAM that must be tuned using observations or model output, which represent processes not resolved by the idealized model. These three tuning coefficients (one in the atmosphere, two in the ocean) are described in the Supplementary material. They are tuned independently for the LOAM simulations with observed mean states and with CM2.1 mean states, as these two systems are fundamentally different. However, the tuning parameters are held constant for all subsequent LOAM experiments using the various CM2.1 mean states. In effect, we assume that these coefficients represent a specific dynamical configuration of the system that is independent of the mean state changes across CM2.1 epochs. In this way, any changes in ENSO in the linearized model are due solely to changes in the mean state fields and not to the tuning parameters.

Given a prescribed set of seasonally varying climatological mean fields (SST, near-surface winds, vertical structure of ocean temperature along the equator, upper ocean currents and upwelling), LOAM simulates the anomalies about the mean state. The underlying assumption in LOAM is that the dynamics of the coupled system in the tropical Pacific are described by linear physics. The coupled atmosphere–ocean variability in the tropical Pacific can then be characterized in terms of the stability, growth rate and

frequency of the system's Floquet modes (eigenmodes of the cyclo-stationary annual propagator matrix). Because the eigenmodes of the coupled system are damped, the model is stochastically forced (as white noise in space and time applied to the SST field). Thompson and Battisti (2001) and Roberts and Battisti (2011) demonstrated that LOAM with observed background states supports a leading mode of the coupled system that has a similar spatial structure, decay rate, and period to that estimated from observations fit to empirical models (Roberts and Battisti 2011). The leading (slowest-decaying) Floquet mode in LOAM is thus referred to as the ENSO mode. Given observed climatological mean states and white noise forcing, LOAM produces reasonably realistic tropical Pacific climate variability, as demonstrated by the spatial structure and variance explained by the leading EOFs of tropical Pacific SSTAs and the seasonal variance and power spectra of SSTAs averaged over the Niño 3 region (5°S – 5°N , 150°W – 90° Roberts 2007; Roberts and Battisti 2011). It has also been shown to capture the character of ENSO in GCMs, and to capture how ENSO can change in the presence of altered mean states (Roberts et al. 2014).

In the present study, we run LOAM with mean fields prescribed from each of three 40-year epochs that were highlighted in Wittenberg (2009), Karamperidou et al. (2014), and Wittenberg et al. (2014), characterized by low (Epoch L), medium (Epoch M) and high (Epoch H) ENSO variance in the CM2.1 pre-industrial control simulation, and investigate the influence of the changes in tropical Pacific mean state on ENSO. These runs are referred to as $\text{LOAM}_{\text{EPOCH L}}$, $\text{LOAM}_{\text{EPOCH M}}$ and $\text{LOAM}_{\text{EPOCH H}}$, respectively. LOAM was also run with mean states prescribed to be the average over all three of these epochs, hereafter referred to as $\text{LOAM}_{\text{CM2.1}}$, as well as from observed mean fields, hereafter referred to as LOAM_{OBS} . In LOAM_{OBS} , the ocean temperature, currents, upwelling and wind stress fields are taken from the UMD Simple Ocean Data Assimilation reanalysis (SODA; Carton and Giese 2008) for the period 1958–2001, and wind fields are taken from the European Centre for Medium-Range Weather Forecast ERA-40 reanalysis (<http://apps.ecmwf.int/datasets/>) for the same period. Stochastic forcing in LOAM is applied by adding a normally distributed random number to each of the spectrally and spatially discretized SST components in the model. The amplitude of the noise forcing is adjusted so that the variance of Niño 3 SST anomalies in LOAM equals that from observations, or from a given epoch of the CM2.1 control simulation. Specifically, three different estimates of the noise amplitude are used in the LOAM experiments: (i) F_{M} , in which the noise amplitude is adjusted so that the Niño 3 variance in LOAM is equal to that during Epoch M; (ii) $F_{\text{CM2.1}}$, in which the noise amplitude is adjusted so that the Niño 3 variance in LOAM is

Table 1 ENSO characteristics in LOAM simulations

LOAM								CM2.1 or obs
Run name	Mean state	Variance tuned to	Noise forcing ampl. (°C) ^a	C_D ^b	Mode period (year) ^c	Mode growth rate (year ⁻¹) ^d	Variance in LOAM ^e	Variance in CM2.1 or obs ^e
LOAM _{EPOCH L} + F _M	Epoch L	–	0.104	1.82E–3	3.2	0.49	2.2	0.7
LOAM _{EPOCH M} + F _M	Epoch M	Epoch M	0.104	1.82E–3	3.0	0.49	1.8	1.8
LOAM _{EPOCH H} + F _M	Epoch H	–	0.104	1.82E–3	3.0	0.43	1.3	3.0
LOAM _{CM2.1} + F _M	Epoch L, M, H avg	–	0.104	1.82E–3	3.0	0.48	1.8	1.7 ^f
LOAM _{CM2.1} + F _{CM2.1}	Epoch L, M, H avg	4000-year CM2.1	0.102	1.82E–3	3.1	0.48	1.7	1.7 ^f
LOAM _{CM2.1} + F _{OBS}	Epoch L, M, H avg	–	0.054	1.82E–3	3.1	0.48	0.5	1.7 ^f
LOAM _{OBS} + F _{OBS}	obs	obs	0.054	1.85E–3	2.8	0.44	0.8	0.8

^aThe amplitude of the noise forcing was prescribed in the following way: F_M was prescribed such that the variance of Niño 3 SSTAs in LOAM_{EPOCH M} matched that in CM2.1 Epoch M, F_{CM2.1} was prescribed such that the variance of Niño 3 SSTAs in LOAM_{CM2.1} matched that over the 4000-yr CM2.1 control run, and F_{OBS} was prescribed such that the variance of Niño 3 SSTAs in LOAM_{OBS} matched that from the last 40 years of observations

^bAtmospheric drag coefficient (see Supplementary material)

^cPeriod of the ENSO mode

^dMode growth rate, expressed as the fractional change in the amplitude of the ENSO mode over the course of a year. Growth rates less than 1 indicate damped modes

^eVariance of 3-month running mean Niño 3 SSTAs

^fVariance of Niño 3 SSTAs across 4000 years of CM2.1

equal to that over the 4000 years of the CM2.1 simulation; and (iii) F_{OBS}, in which the noise amplitude is adjusted so that the Niño 3 variance in LOAM is equal to that from the observed Niño 3 index. The SST output is smoothed with a 1–2–1 filter to reduce the noise, as in Zebiak and Cane (1987) and Thompson (1998a, b). The various LOAM simulations implemented in this study are outlined in Table 1, along with their prescribed mean states and noise forcings.

3 Characteristics of tropical Pacific variability and extreme ENSO epochs in CM2.1

The GFDL CM2.1 global atmosphere/ocean/land/ice model has been widely recognized as a top-performing GCM with regard to its simulation of tropical climate variability, and featured prominently in the third Coupled Model Intercomparison Project (CMIP3) and the Intergovernmental Panel on Climate Change Fourth Assessment Report (Reichler and Kim 2008; van Oldenborgh et al. 2005; Wittenberg et al. 2006). However, like most coupled GCMs, CM2.1 has biases in its ENSO simulation (Wittenberg et al. 2006). These include excessive ENSO variance [Figs. 5a, c, 7 (Takahashi and Dewitte 2016; Wittenberg et al. 2006)] and biased spatial patterns of SST variability, including SST variability that extends too far west, is too equatorially-confined, and is underestimated in the far equatorial eastern Pacific (Fig. 4a, c). Such ENSO biases are common in GCMs, and are likely

tied to tropical Pacific mean state biases (Ham et al. 2013), which in CM2.1 include a cold SST bias along the equator, a warm bias along the coast of South America, and equatorial easterlies that are too broad zonally and extend too far into the western Pacific (Wittenberg et al. 2006).

The 4000 year-long pre-industrial control run of GFDL CM2.1 exhibits large variations in ENSO behavior on multi-decadal time scales, which have been the focus of a number of recent studies (Karamperidou et al. 2014; Wittenberg 2009; Wittenberg et al. 2014). In the control run of this model, the variance of Niño 3 SSTAs during a given 40-year epoch can vary by over a factor of four (from 0.7 to 3.0 °C²; Fig. 1). In this paper we focus on three 40-year periods in the CM2.1 control run that were highlighted in Wittenberg (2009), Karamperidou et al. (2014), and Wittenberg et al. (2014), to represent the diversity of the model's ENSO variability. The time series of Niño 3 SSTAs for each period are shown in Fig. 1b–d. Years 1151–1190 (Epoch L) represent a period of extreme low variability (variance of Niño 3 SSTAs=0.7 °C²). Years 531–570 (Epoch M) are characterized by variability that is similar to the mean of the first 2000 years (variance of Niño 3 SSTAs=1.8 °C²), with fairly normally-distributed Niño 3 SSTAs that have a regular periodicity. Years 1711–1750 (Epoch H) are characterized by numerous intense warm events (variance of Niño 3 SSTAs=3.0 °C²) that are farther apart in time and have less regular periodicity than those in Epoch M.

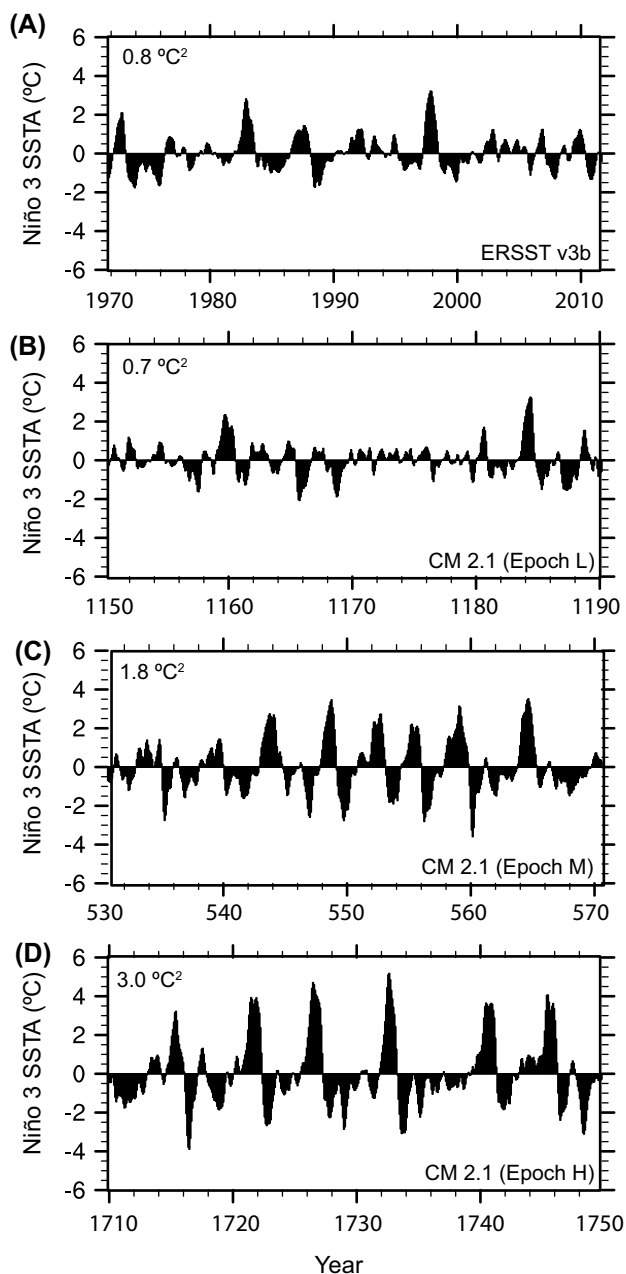


Fig. 1 Time series of 3-month running mean Niño 3 SSTAs in a observations (ERSST.v3b, 1971–2010) and CM2.1 epochs **b** Epoch L, **c** Epoch M, and **d** Epoch H. The variance of each time series is indicated in the top left corner of each panel

The leading patterns of tropical Pacific SST variability in each epoch are shown in Fig. 2. Empirical orthogonal functions (EOFs) 1–3 display roughly similar characteristics across epochs. Notably, a lower fraction of the total variance is explained by the first two EOFs in Epoch L relative to the other epochs and EOFs 2 and 3 appear to be mixed in Epoch M (their eigenvalues are not distinguishable). Figure 3 shows that compared to the long-term variance, the region of maximum variance in Epoch L is

reduced and shifted east, while that in Epoch H is amplified and shifted west.

4 ENSO in a linearized intermediate model versus GFDL CM2.1

As part of our analysis to investigate the sources of the low-frequency ENSO modulation in CM2.1, we employ a linearized anomaly model of the tropical Pacific (LOAM). The rationale for this approach is that it has been shown that all but the strongest observed ENSO events are well represented by linear dynamics (Penland and Sardeshmukh 1995; Roberts and Battisti 2011). Furthermore, comparison of the linear model simulations to the fully nonlinear CM2.1 simulation enables a rough partitioning of the linear and nonlinear components of ENSO evolution in CM2.1.

The LOAM simulation with mean fields prescribed from the CM2.1 climatology averaged over all 120 years of the three epochs ($LOAM_{CM2.1}$), demonstrates spatial and temporal patterns of tropical Pacific SSTA variability that compare well in some aspects to CM2.1, while other features are notably dissimilar (Figs. 4, 5, 6, 7). Differences include the region of maximum variance, which does not extend as far west in $LOAM_{CM2.1}$ and is broader meridionally and weaker near the eastern boundary than in CM2.1 (c.f. Fig. 4c, d). In addition, Niño 3 SSTAs in CM2.1 display large asymmetry in the amplitude of warm versus cold events (Figs. 5c, 6), indicating the presence of strong nonlinearities in CM2.1 (Choi et al. 2013, 2015). In contrast, Niño 3 SSTAs in $LOAM_{CM2.1}$ are linear by construction (Figs. 5d, 6). The power spectrum of Niño 3 SSTAs in the first 2000 years of CM2.1, much like the observations, shows a broad spectral peak between 2 and 5 year (median period 3.4 year), while the power spectrum in $LOAM_{CM2.1}$ is much more sharply peaked (median period 3.2 year; Fig. 7). These results suggest that ENSO nonlinearities and/or multiplicative noise, which are not included in LOAM, may be important contributors to the temporal and spatial structure of ENSO in CM2.1.

In nature, ENSO is strongly synchronized to the calendar year, with ENSO events tending to peak in boreal winter (Fig. 8a). In contrast, ENSO in CM2.1 displays weak seasonality, with Niño 3 SSTA variance peaking in boreal summer (Fig. 8c). Given CM2.1 mean states, ENSO in LOAM displays a notably distinct seasonality from CM2.1, with variance reaching a minimum in May/June and peaking around Sept. (Fig. 8d). The differences in seasonality between $LOAM_{CM2.1}$ and LOAM tuned to observations ($LOAM_{OBS}$, panels b and d in Fig. 8) are likely related to the biased annual cycle in CM2.1, through its influence on the seasonal growth rate of ENSO. In particular, the CM2.1 climatological wind field features an overly muted

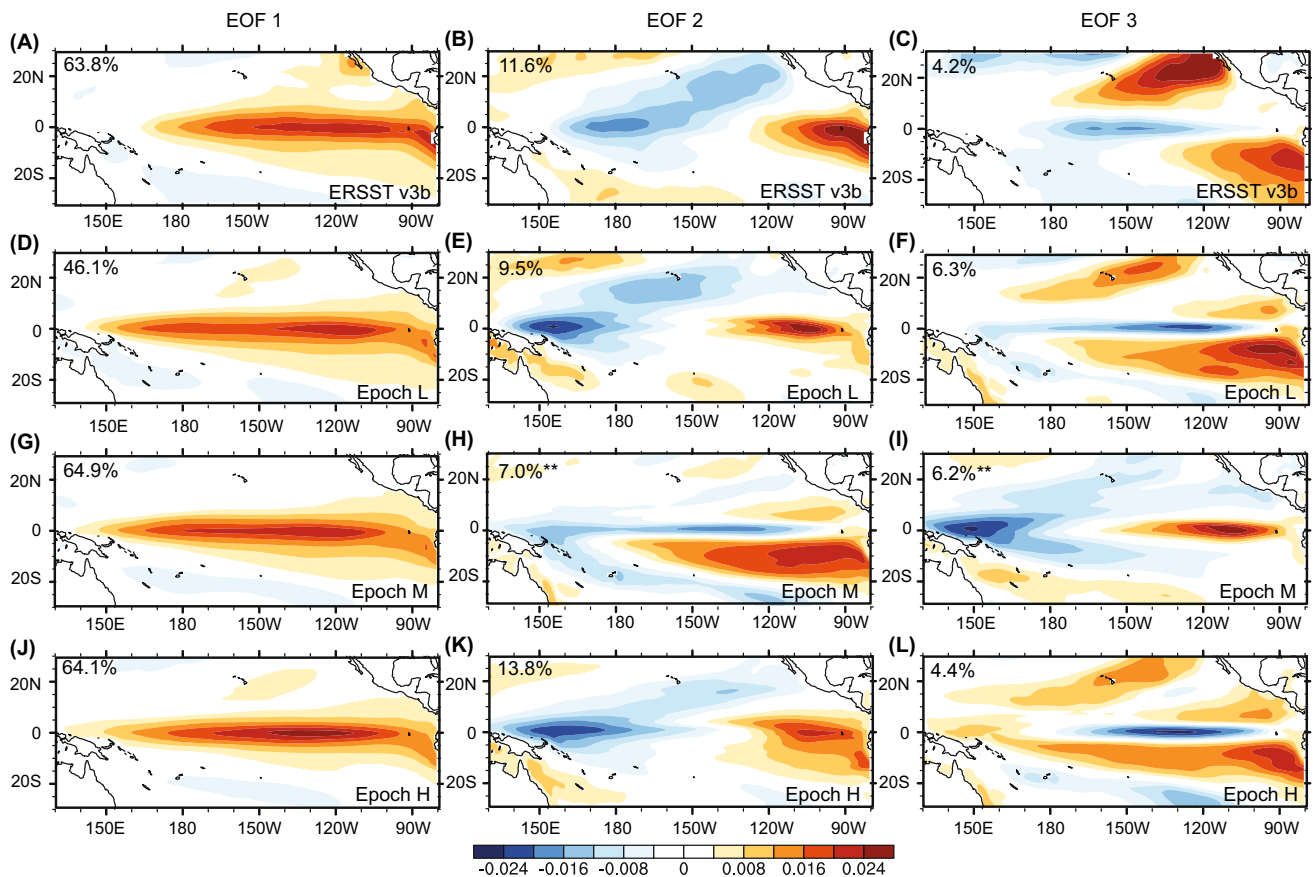


Fig. 2 Normalized EOF 1–3 of tropical Pacific SSTAs from **a–c** detrended observations (ERSST.v3b, 1971–2010) and CM2.1 epochs **d–f** Epoch L, **g–i** Epoch M, and **j–l** Epoch H. The fraction of total

SSTA variance captured by each pattern is indicated in the top left corner of each panel. **EOF 2 and 3 in Epoch M are not statistically distinguishable, based on the method of North (1982)

and delayed relaxation of the trades during boreal spring and an enhancement of the trades during boreal summer and fall that is too strong and does not persist into the winter. These trade wind biases are associated with a stronger semi-annual cycle in the tropical Pacific than is observed (Wittenberg 2009).

These results indicate that LOAM is able to capture some, but not all of the important features of ENSO behavior in CM2.1. Shortcomings of LOAM include the absence of surface heat flux dependence on wind speed (which may account for the difference in SST variability in the western Pacific and in the subtropics in CM2.1 versus LOAM; c.f. Fig. 4c, d). In addition, LOAM omits all nonlinear dynamics, including nonlinear dependence of atmospheric heating and wind stress anomalies on SST anomalies and nonlinear ocean dynamics (Chen et al. 2016; Choi et al. 2013; Takahashi and Dewitte 2016). However, that LOAM has successfully managed to capture many of the fundamental characteristics of observed ENSO (Roberts and Battisti 2011; Thompson and Battisti

2001) as well as capture changes to ENSO due to mean state changes in other CGCMs (Roberts et al. 2014) suggests that the inability of LOAM to characterize some of the important features of ENSO in CM2.1 is because CM2.1's ENSO does not conform to the assumptions that are in LOAM, e.g. due to the strong nonlinearities in CM2.1.

Given the success of LOAM in simulating many observed features of ENSO variability, the linear model provides an excellent opportunity to contrast the linear components of ENSO evolution with the full nonlinear evolution in CM2.1. It also provides insight into how the mean state contributes to the (linear component of the) differences in variance between the L, M, and H epochs. We thus use LOAM to evaluate the linear component of the ENSO dynamics, sensitivities, and feedbacks in CM2.1. While this linear component is dominant in observations, it appears to be less so in CM2.1. The misfit of LOAM's ENSO to CM2.1's ENSO is then one measure of the importance of nonlinearities in CM2.1.

Fig. 3 Variance of tropical Pacific SSTAs in **a** 500 years of the CM2.1 control run and the CM2.1 epochs **b** Epoch L, **c** Epoch M, and **d** Epoch H. In subpanels **(e-h)**, the variances are normalized with respect to the maximum in *each plot*

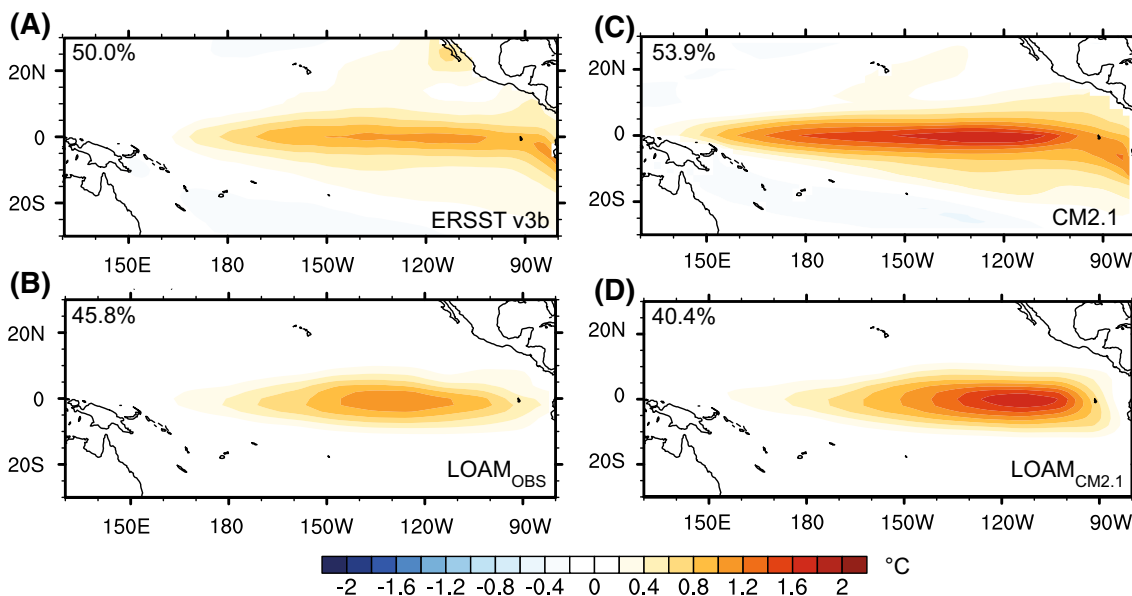
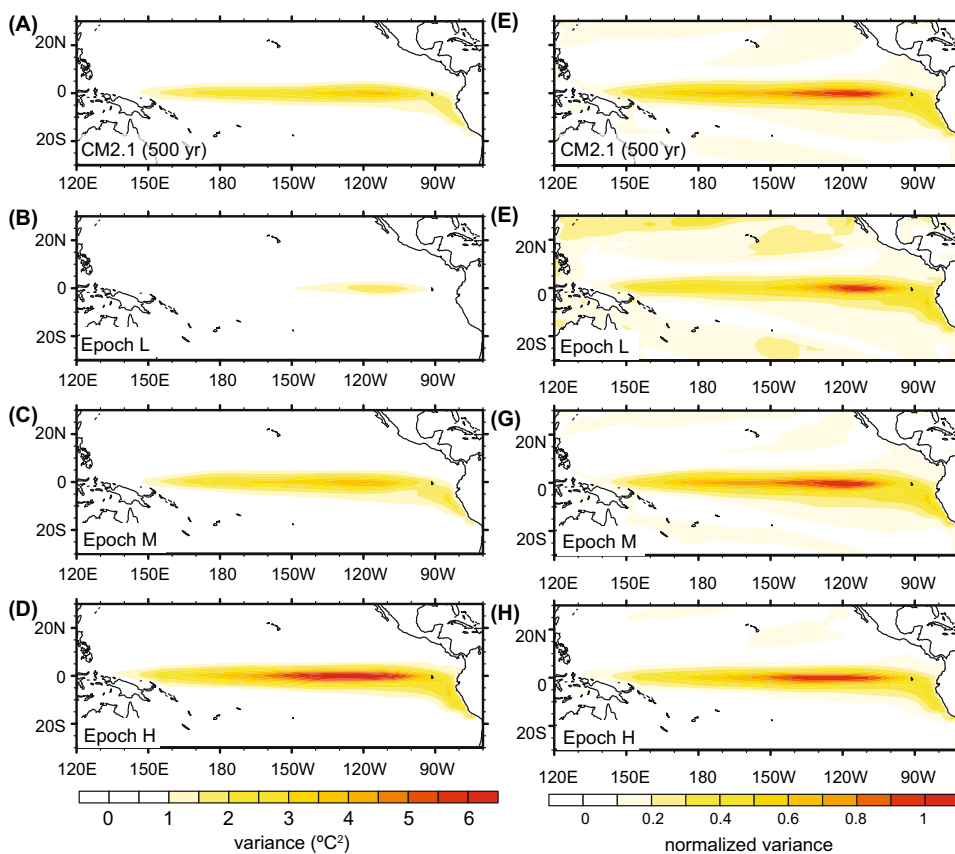


Fig. 4 EOF 1 of tropical Pacific SSTAs from **a** observations (ERSST.v3b, 1971–2010), **b** 200 years of LOAM run with observed mean fields, **c** 200 years of the CM2.1 control-run simulation, and

d 200 years of LOAM run with mean fields from CM2.1 (averaged over Epoch L, M, H). The fraction of total SSTA variance captured by EOF 1 is indicated in the *top left corner of each panel*

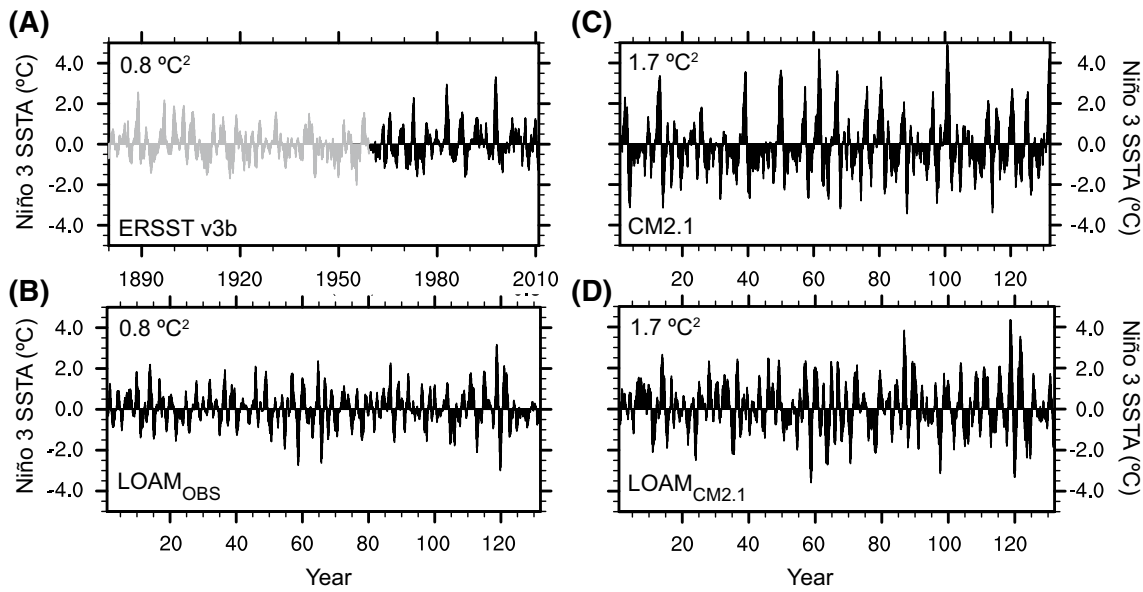


Fig. 5 Three-month running mean Niño 3 SSTAs in **a** observations (ERSST.v3b, 1880–2010), **b** 130 years of the 4000-year LOAM with mean states from observations, **c** 130 years of the 4000-year control run of CM2.1, and **d** 130 years of the 4000-year LOAM with mean states from CM2.1 (averaged over Epoch L, M, H). The variance of

each complete time series is indicated in the *top left corner* of each panel. Only the last 50 years of observational data was used to calculate the variance in panel (a), as only the period from 1961 to 2010 was used to tune the LOAM_{OBS} run

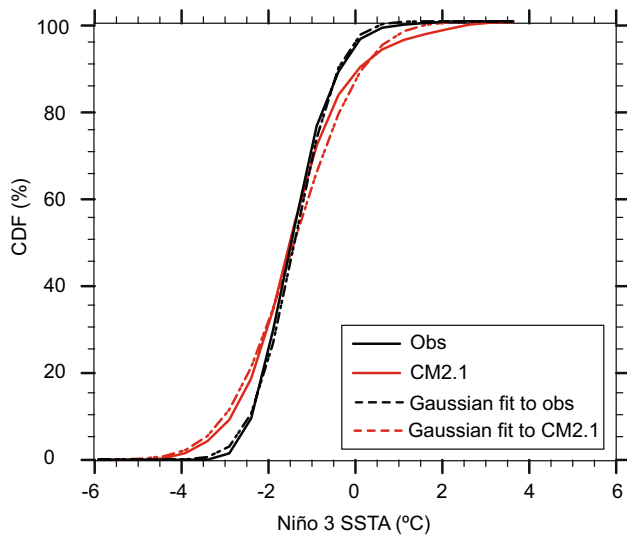


Fig. 6 Cumulative probability distributions of Niño 3 SSTAs in detrended observations (*black*; NOAA ERSST v3b, 1880–2011 AD) and 2000 years of the CM2.1 control run (*red*). Gaussian distributions with the mean and standard deviation estimated from the data are plotted as *dashed lines*. The LOAM_{OBS} and LOAM_{CM2.1} curves have been omitted for clarity, but overlay the Gaussian distributions fit to observations and CM2.1, respectively

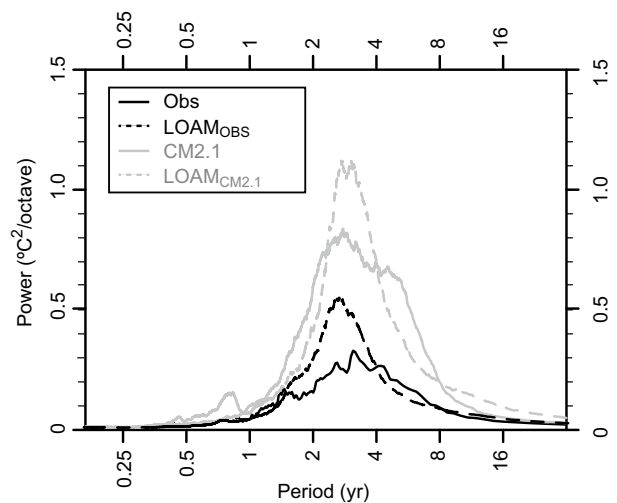
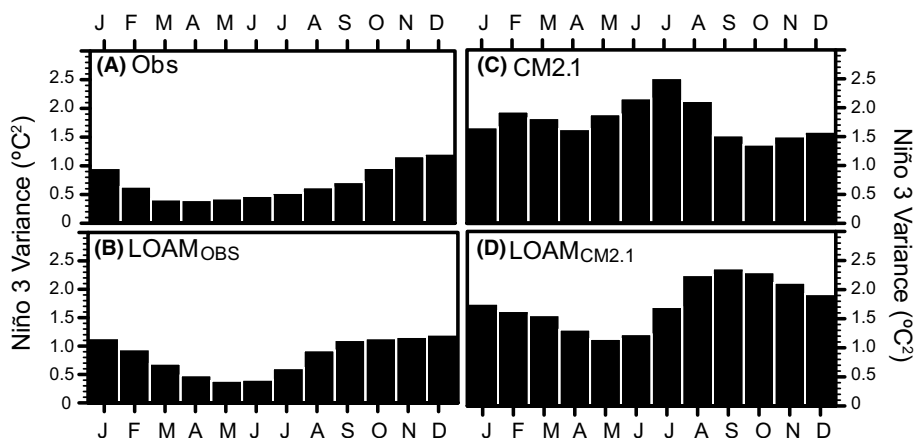


Fig. 7 Power spectra of 3-month running mean Niño 3 SSTAs in observations (*solid black*; NOAA ERSST.v3b, 1880–2011), the 4000-year LOAM tuned to observations (*dashed black*), the 4000-year control run of CM2.1 (*solid grey*) and the 4000-year LOAM tuned to CM2.1 (*dashed grey*). The power spectra were computed using a forward Fast Fourier Transform and preserve variance so that the area under the curve equals the variance of the detrended Niño 3 time-series

Fig. 8 Variance of 3-month running mean Niño 3 SSTAs as a function of month in **a** observations (ERSST.v3b, 1880–2010), **b** the 4000 year LOAM with observed mean states, **c** the 4000 year CM2.1 control run, and **d** the 4000 year LOAM run with CM2.1 mean states



5 Drivers of low frequency ENSO modulation in CM2.1

Because the CM2.1 control simulation is unforced, there are essentially four, non mutually exclusive, mechanisms that could cause the large multi-decadal ENSO variability: (1) low frequency changes in the tropical Pacific mean state, which alter the stability of the ENSO system; (2) low frequency changes in stochastic (weather) processes that influence ENSO; (3) random sampling from a stationary, linear process; and (4) nonlinear dynamics, including multiplicative noise, in the ENSO system that spreads variance over a range of time scales—e.g. nonlinear interaction between the annual cycle and internal modes of variability in the tropical Pacific that produce deterministic chaos (see e.g. Timmermann et al. 2002). We discuss each of these possible mechanisms, below:

5.1 Influence of tropical Pacific mean state changes on ENSO in the linear model

In their examination of the multi-decadal rectification of ENSO modulation in CM2.1, Ogata et al. (2013) demonstrated that mean state changes during the different CM2.1 epochs may be generated by the extreme ENSO behavior (that is, they are the residual impact of the ENSO cycles during each epoch), as also suggested by Vimont (2005), Wittenberg (2009), and Wittenberg et al. (2014). On the other hand, the concept that ENSO is highly sensitive to mean state changes in the tropical Pacific has been widely explored and demonstrated, typically in studies that invoke intermediate complexity models of varying descriptions (Battisti and Hirst 1989; Dewitte 2000; Roberts et al. 2014; Wittenberg 2002; Zebiak and Cane 1987). It has further been suggested that the post-1970’s shift in ENSO characteristics may be related to changes in the tropical Pacific background state (An and Wang 2000).

We sought to evaluate the impacts of the tropical Pacific mean state changes in CM2.1 on ENSO by prescribing the annual cycle of tropical Pacific climatology

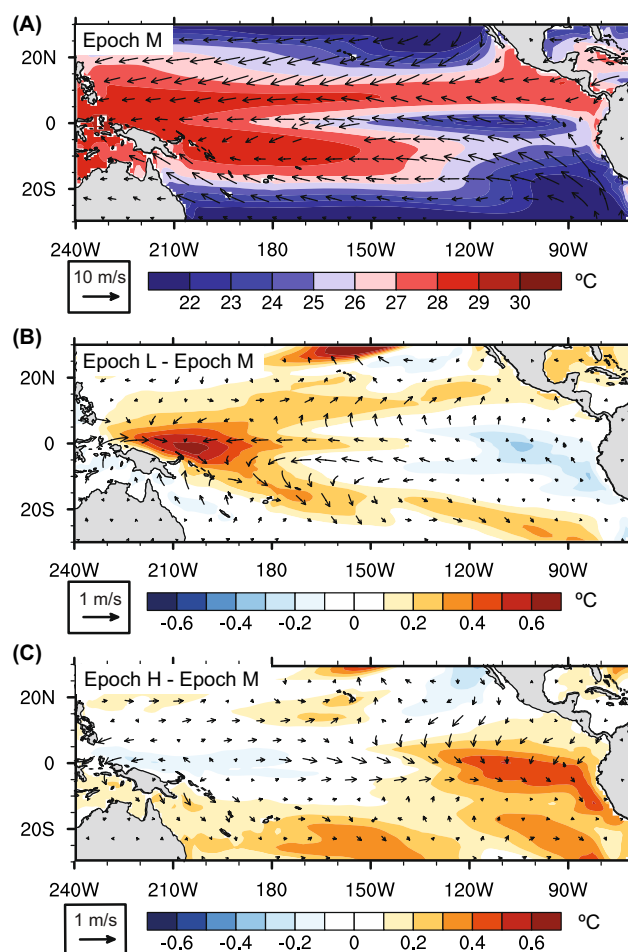


Fig. 9 **a** Mean annual tropical Pacific SST and near-surface winds in CM2.1 Epoch M and differences in mean surface winds between CM2.1 epochs: **b** Epoch L–M; **c** Epoch H–M

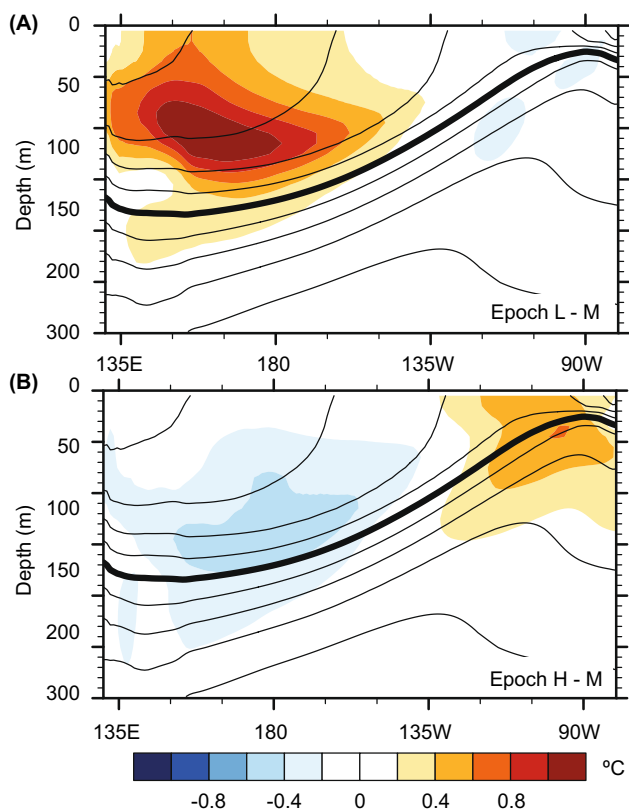


Fig. 10 Difference in mean annual equatorial Pacific upper ocean temperature (colors; averaged between 2°S:2°N) between CM2.1 epochs: **a** Epoch L–M and **b** Epoch H–M. Unfilled contours are the mean annual equatorial temperature in Epoch M. The contour interval is 2 °C and the bold contour is the 20 °C isotherm

averaged separately over the three representative CM2.1 epochs in LOAM. The differences in annually-averaged tropical Pacific climatology among these epochs are shown in Figs. 9 and 10. Progressing from Epoch L to Epoch H, the mean states are characterized by weakening of the surface easterly trade winds in the western and central equatorial Pacific, warming of the ocean surface and subsurface in the eastern equatorial Pacific, and cooling in the western equatorial Pacific (Figs. 9, 10)—consistent with the results of Ogata et al. (2013) in their examination of the multi-decadal rectification of ENSO modulation in CM2.1.

When the mean states from the three CM2.1 epochs are prescribed in LOAM, the relative changes in the variance of Niño 3 SSTAs in the linear model are opposite to those observed in the CM2.1 simulation: the variance is lowest in Epoch H and highest in Epoch L (Table 1; Fig. 11). In Epoch H, the decreased ENSO variance relative to Epoch M is due to a decrease in the growth rate of the ENSO mode. In Epoch L, the increase in variance relative to Epoch M is tied to the increased growth rate of the lower order coupled modes (not shown). Collectively, these

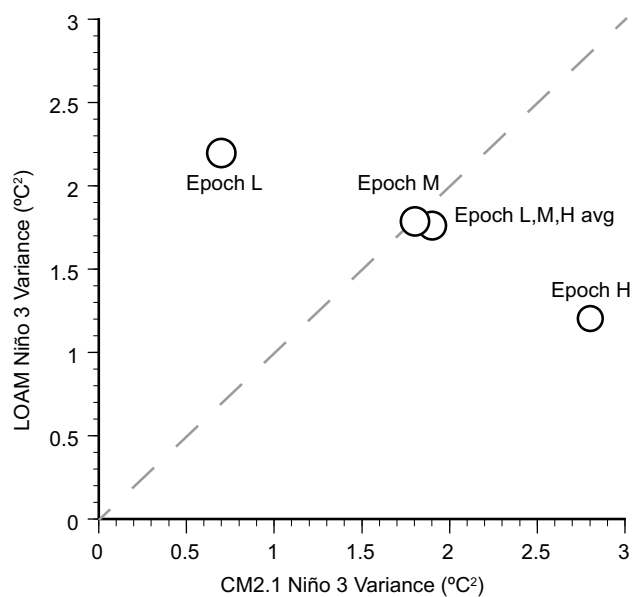


Fig. 11 Variance of Niño 3 SSTAs in LOAM versus CM2.1. The LOAM simulations correspond to $LOAM_{EPOCH L+F_M}$, $LOAM_{EPOCH M+F_M}$, $LOAM_{EPOCH H+F_M}$ and $LOAM_{CM2.1+F_M}$ in Table 1. The diameter of the data points is proportional to the growth rate of the ENSO mode. The dotted 1:1 line is plotted for visual reference

results indicate that tropical Pacific mean state changes are not the primary cause of the intrinsically-generated extreme ENSO epochs in the CM2.1 control run.

The LOAM simulations demonstrate the sensitivity of the linear component of ENSO to changes in the tropical Pacific mean state (Table 1) and provide evidence for a two-way feedback mechanism between low frequency ENSO modulation and tropical Pacific mean state changes in CM2.1, wherein: (1) stochastic forcing and nonlinearity produce low frequency ENSO modulation, which rectify into tropical Pacific mean state changes due to the ENSO asymmetries in CM2.1; (2) these rectified mean state changes then feed back negatively on the ENSO growth rates, thus tempering the ENSO modulation. For example, as shown in Ogata et al. (2013), strong-ENSO epochs in CM2.1 weaken the multi-decadal zonal SST gradient and zonal winds in the central to western equatorial Pacific (Fig. 9c), and thus weaken the zonal tilt of the thermocline (Fig. 10b). According to the stability analysis performed with LOAM, these mean state changes act to stabilize the coupled system and weaken ENSO (Table 1). Along the same lines, weak-ENSO epochs in CM2.1 strengthen the multi-decadal zonal SST gradient and zonal wind stress in the central to western equatorial Pacific (Fig. 9b), and thus strengthen the zonal tilt of the thermocline (Fig. 10a). The LOAM stability analysis indicates that these mean

state changes act to destabilize the lower order modes (not shown) and thereby modestly strengthen the ENSO variability (Table 1; Fig. 11).

Further experiments were performed with LOAM, in which individual components of the mean states of Epochs H and L were substituted into the Epoch M simulation. Results from these experiments (not shown) indicate two primary mechanisms of increased stability of the coupled system in Epoch H. First, the weaker climatological trade winds lead to reduced ocean-atmosphere coupling via the linear dependence of the wind stress anomalies on the mean wind speed in LOAM (see Eq. 18 in Supplemental material; Battisti and Hirst 1989). Second, a weaker mean zonal tilt of the equatorial thermocline leads to weaker contribution of anomalous upwelling to SST changes (i.e. weakened upwelling feedback; see Eqs. 1–3 in the Supplementary material). Details of these feedback processes can be found in Thompson (1998a, b) and Roberts and Battisti (2011). The primary mechanisms of decreased stability of the coupled system in Epoch L are the same as those discussed above, only with opposite sign (e.g. stronger climatological winds enhance coupling).

There are two caveats to the proposed negative feedback mechanism between the tropical Pacific mean state changes and low frequency ENSO modulation in CM2.1. First, nonlinearities in CM2.1 may act to compensate for these large “mean state induced” changes in the linear stability, thereby tempering the sensitivity of ENSO to mean state changes. Second, because LOAM does not include state-dependent noise forcing, any influence that the mean state changes may have on the noise forcing are not considered in this analysis.

5.2 Influence of changes in atmospheric noise on low-frequency ENSO modulation

The results highlighted in the previous section suggest that mean state changes in the tropical Pacific do not explain the periods of extreme ENSO variability in CM2.1—suggesting that the ENSO modulation in CM2.1 is instead driven by atmospheric noise and/or nonlinear dynamics. These results are consistent with the results presented in Wittenberg et al. (2014), who showed that the occurrence of extreme-ENSO epochs in CM2.1 were in fact unpredictable.

Multi-decadal fluctuations of ENSO variability could arise through low frequency changes in the structure and/or amplitude of the atmospheric noise forcing (either internal or external to the tropical Pacific), including a multiplicative dependence of westerly wind bursts on the zonal extent of the Pacific warm pool (Graham et al. 2016). While an attempt was made to characterize the noise forcing in the three CM2.1 epochs using a Linear Inverse Model (LIM;

e.g. Penland and Sardeshmukh 1995), it was concluded that 40 years of CM2.1 data was not long enough to robustly constrain the dynamics of the coupled system (see S.2 in the Supplemental material for details). These results are in contrast to those from (Newman et al. 2011), in which 42 years was deemed sufficient to constrain a LIM trained on observational data. These results again highlight the difference between ENSO in CM2.1 and ENSO in nature—the LIM fit to CM2.1’s strongly-modulated ENSO system is less robust to short epochs than the LIM fit to observations. Because of these issues, the possible role of changes in atmospheric noise forcing on CM2.1’s ENSO modulation has yet to be evaluated.

5.3 Low-frequency ENSO modulation through randomly sampling a stationary, linear process

Independent from any changes in the background climate state or changes in the structure or amplitude of atmospheric noise forcing, multi-decadal fluctuations in ENSO variability can arise solely from a system governed by linear, stationary dynamics. For a stationary, linear process with well-defined long-term variance, and for epochs that randomly and independently sample the underlying distribution of multi-decadal ENSO variance, the probability distribution function (PDF) of epochal variance will match that of a χ^2 distribution (Russon et al. 2014).

In order to compare a χ^2 distribution to the ENSO modulation present in CM2.1, the probability distribution of ENSO variance (hereafter defined as the variance of Niño 3 SSTAs) in 40-year intervals was plotted from the first 2000 years of the CM2.1 simulation alongside χ^2 distributions (Fig. 12), calculated using Eqs. 1–2, below (from Russon et al. 2014). To further compare CM2.1’s ENSO modulation with that of a linear system with additive noise, the 2000-year LOAM simulation with CM2.1 mean states and CM2.1-tuned noise, and the 2000-year LOAM simulation with observed mean states and observation-tuned noise were also plotted.

While one might expect the temporal properties of ENSO in the low-dimensional, linear system in LOAM to be notably distinct from the high dimensional, fully nonlinear CM2.1, the distribution of multi-decadal ENSO variance is notably similar in CM2.1 and the linear model, with the exception of a slightly broader distribution in CM2.1 (Fig. 12a). A two-sample Kolmogorov–Smirnov test of the variance histograms indicates that the null hypothesis (that the two data sets were drawn from the same distribution) cannot be rejected. The correspondence of the CM2.1 histogram with the χ^2 distribution indicates that ENSO statistics even in the highly nonlinear CM2.1 are roughly stationary at multi-decadal time scales. This

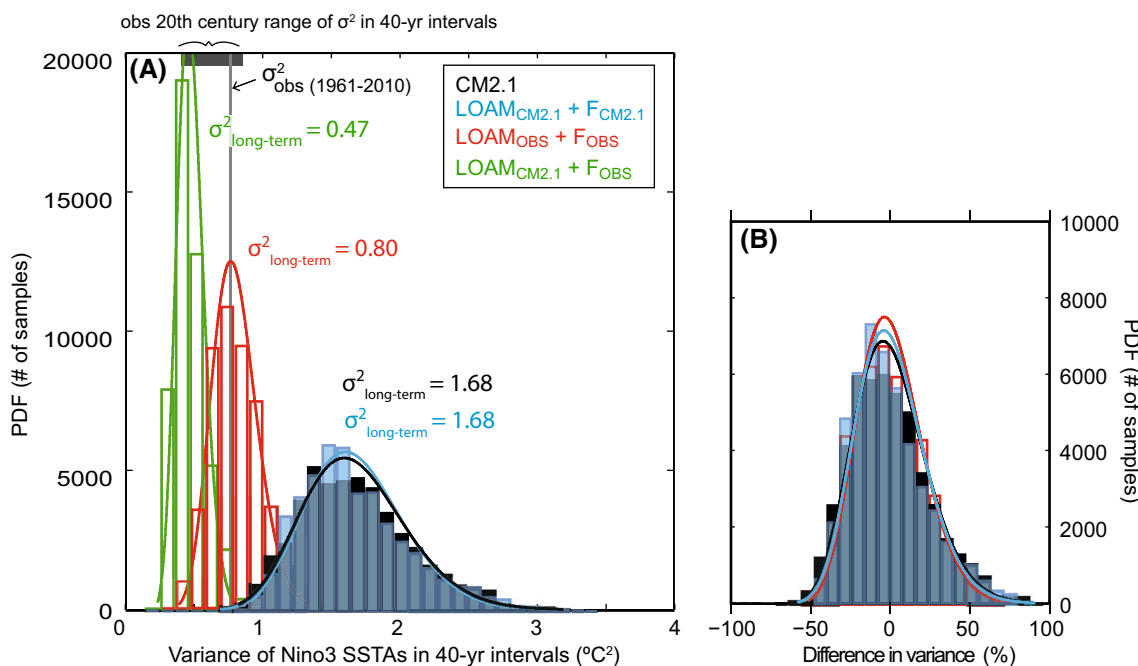


Fig. 12 Probability distributions of 40-year variance of Niño 3 SSTs (bars) plotted with χ^2 distributions (lines) for the 4000-year CM2.1 run (black), the 4000-year LOAM_{CM2.1}+F_{CM2.1} run (blue), the 4000-year LOAM_{OBS}+F_{OBS} run (red), and the 4000-year LOAM_{CM2.1}+F_{OBS} run (green). The χ^2 distributions were calculated using Eqs. (1)–(2). The grey shaded bar represents the range

of observed variance in 40-year intervals across the twentieth century and the vertical line represents the observed variance during the period 1961–2010 (from NOAA ERSST v3b). **b** PDFs from subpanel (a) converted into relative differences in variance, with respect to the long-term variance in each simulation

result is consistent with the finding by Wittenberg (2009) and Wittenberg et al. (2014) who showed that the warm events in CM2.1 resembled a memory-less interannual process with no decadal-scale predictability. These findings demonstrate that the low-frequency ENSO modulation in CM2.1 is driven by transient processes that operate at time scales that are interannual or shorter.

Like most coupled GCMs, CM2.1 has biases in its ENSO simulation (Wittenberg et al. 2006). Importantly, these biases include excessive ENSO variance in CM2.1 [Figs. 5a, c, 7 (Takahashi and Dewitte 2016; Wittenberg et al. 2006)]. In order to evaluate the influence of this overly strong ENSO variance on the low-frequency ENSO modulation, the variance distribution from the LOAM simulation tuned to observations (LOAM_{OBS}+F_{OBS}; red histogram in Fig. 12) was compared to the distribution from the LOAM simulation tuned to CM2.1 (LOAM_{CM2.1}+F_{CM2.1}; black histogram in Fig. 12). The results demonstrate that the distribution with weaker ENSO variance (LOAM_{OBS}+F_{OBS}) is much more sharply peaked about its respective mean than the distribution with stronger ENSO variance (LOAM_{CM2.1}+F_{CM2.1}). Indeed, the range of multi-decadal variance in CM2.1 (and LOAM tuned to CM2.1) is twice that produced by LOAM tuned to observations.

There is a simple statistical reason for this, which explains how CM2.1’s strong ENSO variance is directly related to its strong inter-epoch modulation of ENSO variance (Fig. 12). Given a normal distribution with variance σ^2 , the expected distribution of the sample variance of a random sample of size n is

$$s^2 = \frac{\sigma^2 \chi_{n^*-1}^2}{n^* - 1} \tag{1}$$

where $\chi_{n^*-1}^2$ is the Chi square distribution with n^*-1 degrees of freedom. n^* can be estimated from:

$$n^* = \frac{n}{\tau_d}; \quad \tau_d = 1 + \sum_{i=1}^L \rho_i^2 \tag{2}$$

where τ_d is a dimensionless factor by which the effective degrees of freedom are reduced relative to the number of data points in each interval (here, $n = 480$) and is constrained by the autocorrelation of the Niño 3 SSTA data. The autocorrelation function (ρ) is summed over the number of time steps (L) needed to reach the first two sign changes in the autocorrelation function (von Storch and Zwiers 2003; Russon et al. 2014). Now suppose that ENSO is memoryless beyond a few years—as in CM2.1, in which the wait times between El Niño events

are Poisson-distributed at decadal and longer scales (Wittenberg 2009), with no apparent decadal predictability of ENSO amplitude (Wittenberg et al. 2014). Further suppose that the Niño 3 SST anomalies have long-term variance σ^2 , and that each 40-year epoch contains n^* effectively-independent samples of the Niño 3 SST anomalies. The inter-epoch spread of the epochal variance, i.e. the variance modulation, would then increase like the square of the long-term variance σ^2 :

$$\text{Var}(s^2) = \left(\frac{\sigma^2}{n^* - 1}\right)^2 \text{Var}(\chi_{n^*-1}^2) = \left(\frac{\sigma^2}{n^* - 1}\right)^2 2(n^* - 1) = \frac{2\sigma^4}{(n^* - 1)} \quad (3)$$

In simple terms, a weak memoryless ENSO can only exhibit weak variance, while a strong memoryless ENSO can exhibit either strong or weak variance—resulting in much more variance modulation. This disparity is largely removed if the relative change in variance (with respect to the long-term variance) is compared instead (Fig. 12b). In this case the empirical distributions are highly similar, and thus a -40 to $+55\%$ change in ENSO variance in a given 40-year interval (representing 2.5–97.5% of the CM2.1 distribution) is similarly likely in the CM2.1, LOAM_{CM2.1} and LOAM_{OBS} simulations.

To summarize: these results indicate that the distribution of ENSO variance in CM2.1 is dramatically broadened with respect to the linear system with ENSO variance tuned to that observed over the past 50 years. However, the broad CM2.1 distribution is entirely consistent with the distribution expected from a linear system that has excessive ENSO variance. The correspondence of the CM2.1 histogram with that from the linear model and the χ^2 distribution indicates that ENSO statistics in CM2.1 are roughly stationary at multi-decadal time scales, demonstrating that the low-frequency ENSO modulation in CM2.1 is driven by transient processes that operate at time scales that are interannual or shorter. Taken together, the results from the linear LOAM and nonlinear CM2.1 show that a memory-less interannual ENSO, whether linear or highly nonlinear, will generate interdecadal variance modulation that resembles a χ^2 distribution, and that the variance modulation increases sharply as ENSO strengthens. In this way, CM2.1's overly strong ENSO variance directly contributes to its strong multi-decadal modulation. In absolute terms, the multi-decadal modulation in CM2.1 is twice that produced by a linear system tuned to the ENSO variance observed over the past 50 years. In contrast, the relative changes in ENSO modulation are notably similar between the linear and nonlinear models, with the exception of a slightly broader distribution in the nonlinear CM2.1. These results underscore the findings of Russon et al. (2014) that only relative changes in multi-decadal ENSO variance can robustly be compared across models and observations.

5.4 The influence of nonlinearities on low-frequency ENSO modulation in CM2.1

While the results presented in Sect. 5.3 demonstrate that the nonlinearities in CM2.1 do not dramatically broaden the distribution of variance as compared to a linear system with equal ENSO variability, this does not imply that nonlinearities are entirely unimportant in determining the multi-decadal modulation of ENSO. The nonlinearities may in fact be critical to the multi-decadal ENSO modulation by contributing to the overly active ENSO variability that causes the enhanced multi-decadal modulation, e.g. through enhancing the growth of strong El Niño events (e.g. Takahashi and Dewitte 2016).¹ Additional simulations with LOAM suggest that linear dynamics operating on the biased CM2.1 mean states are not the source of the overactive ENSO activity in CM2.1 (see S.3 in the Supplementary material)—which in turn further suggests that nonlinear dynamics and multiplicative noise likely play an important role in driving the excessive ENSO variance, and thus low-frequency ENSO modulation, present in CM2.1. Results presented below indeed demonstrate that these nonlinearities are inextricably linked to the low-frequency ENSO modulation in CM2.1.

The coupled ocean–atmosphere system appears to be substantially more nonlinear in CM2.1 than has been observed over the past 50 years (Figs. 13, 14). A key nonlinearity in CM2.1 is the response of the central Pacific low-level wind (and zonal wind stress) anomalies to SST anomalies—indicative of the Bjerknes feedback that is central to the physics of ENSO (Battisti and Hirst 1989). This feedback is approximately linear for all but the strongest El Niño events in the observations, while a highly nonlinear feedback is present in CM2.1 (Fig. 13, S2). These results suggest that the highly nonlinear response of the atmosphere to central Pacific SST anomalies may be responsible for the growth of strong El Niño events in CM2.1.

Previous studies have also suggested that the key nonlinearities relevant to ENSO in CM2.1 are in the atmosphere (Chen et al. 2016; Choi et al. 2013; Takahashi and Dewitte 2016). Possible sources of the nonlinear response

¹ However, it is also possible that the strong nonlinearity in CM2.1 is a symptom, rather than a cause of its strong ENSO variability. The strong climatological cold tongue in CM2.1 suggests that the model has overactive ocean-dynamical cooling. If this is indeed the case, hyperactive (but possibly still linear) subsurface ENSO feedbacks may be the driver of its higher amplitude SSTAs. In a model with a climatological equatorial cold bias (which shifts the atmospheric convective zones farther to the west and farther off-equator), those greater SSTAs then produce a greater atmospheric nonlinearity (Choi et al. 2013).

Fig. 13 Monthly zonal wind stress anomalies in the western Pacific (left column) and central Pacific (right column) versus Niño 3 SSTs in 500 years of the CM2.1 control simulation (top row) or observations (bottom row; 1958–2001; SODA zonal windstress and ERSST v3b SST data). The CM2.1 data are divided into two subsets—the “high variance epochs” subset contains data from periods in which the 40-year running mean variance of Niño 3 SSTs $\geq 2.0^\circ\text{C}^2$, while the “low variance epochs” subset contains data from periods in which the 40-year running mean variance of Niño 3 SSTs $\leq 1.0^\circ\text{C}^2$. For the WP data (left column) zonal wind anomalies were averaged over the Niño 4 region (160°E:150°W, 5°S:5°N) for observations and over 150°E:160°W, 5°S:5°N for CM2.1 (representing the region of peak zonal wind anomalies in each data set). For the CP data (right column), the zonal wind anomalies were averaged over the Niño 3.4 region (170°W:120°E, 5°S:5°N) for both CM2.1 and observations

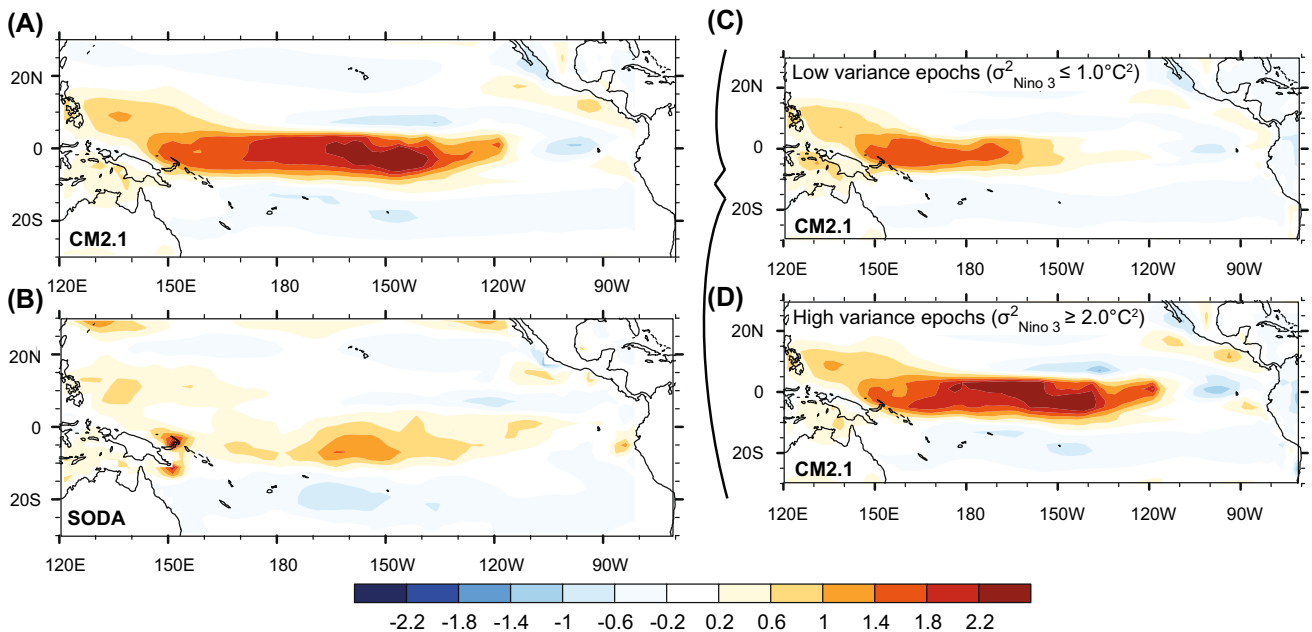
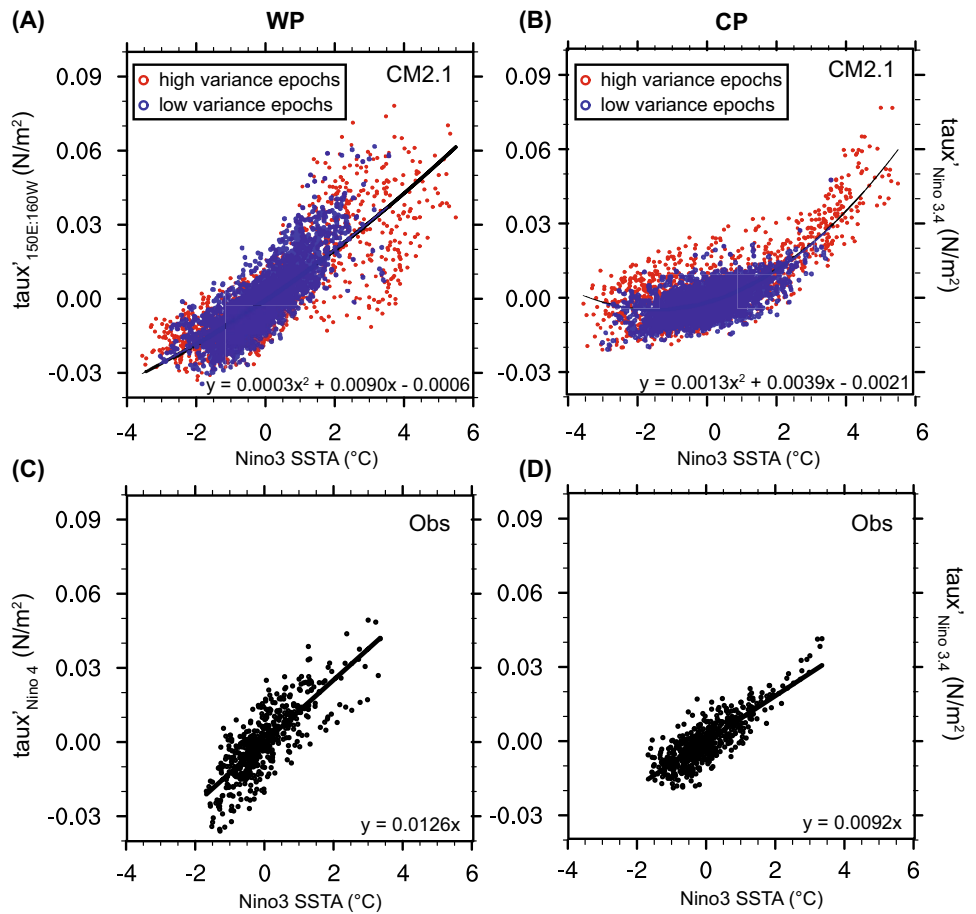


Fig. 14 Skewness of tropical Pacific zonal wind stress anomalies in **a** 500 years of the CM2.1 control simulation; **b** observations (SODA v2.0.2-4, 1958–2007); **c** low variance epochs in CM2.1 and **d** high variance epochs in CM2.1. The CM2.1 data are divided into two subsets—the “low variance epochs” subset **c** contains data from peri-

ods in which the 40-year running mean variance of Niño 3 SSTs $\leq 1.0^\circ\text{C}^2$ while the “high variance epochs” subset **d** contains data from periods in which the 40-year running mean variance of Niño 3 SSTs $\geq 2.0^\circ\text{C}^2$

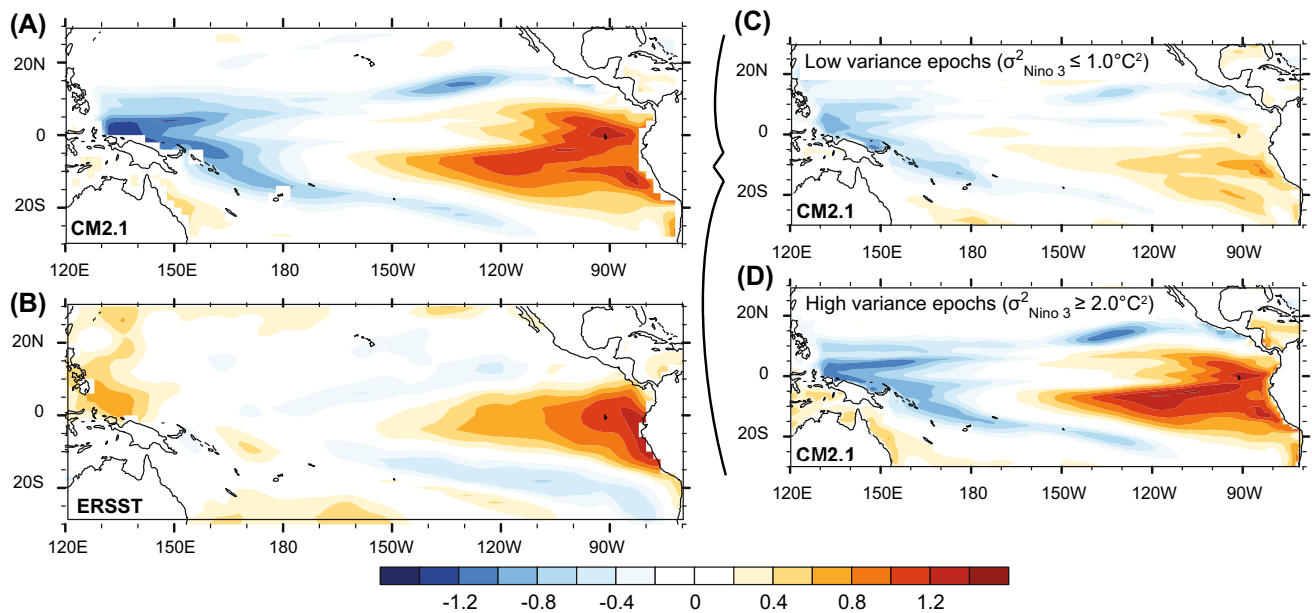


Fig. 15 As in Fig. 14, but for SSTAs. Observational data is from ERSST.v3b, for the period 1951–2010

of the atmosphere to SST anomalies in CM2.1 include a nonlinear moisture convergence feedback, changes in the character of the central Pacific atmospheric boundary layer associated with shifts in the edge of the warm pool convective region, the nonlinear relationship between specific humidity and surface air temperature in the tropics, and state-dependent multiplicative noise forcing (e.g. the eastward shift of westerly wind events, as the warm pool shifts eastward during the onset of El Niño events; Graham et al. 2016; Levine 2016; Vecchi et al. 2006; see S.4 in the Supplementary material for further discussion). Each of these nonlinearities may be amplified by the background state biases in the Pacific in CM2.1, including an excessive contrast between the off-equatorial convergence zones (which are too rainy) and the eastern equatorial cold tongue (over which the atmosphere is too clear and dry). This enhanced contrast could strengthen the atmospheric nonlinearity near the equator, by giving convection more room to increase during El Niño and less room to decrease during La Niña (Chen et al. 2016). Whatever the source(s) of the overly nonlinear Bjerknes feedback in the central Pacific in CM2.1, it appears to give rise to larger ENSO events than those yet observed.

Evidence for an important role of such transient nonlinearities in driving the low-frequency ENSO modulation in CM2.1 can be seen by evaluating the SST and wind/wind-stress anomalies separately for the high- and low-variance ENSO epochs. High-variance ENSO epochs in CM2.1 are populated by more extreme ENSO events (panels a and b of Fig. 13), which are governed by a highly nonlinear Bjerknes feedback in the central Pacific. The threshold behavior of

zonal wind and wind stress anomalies in the central Pacific during these epochs in response to warm SST anomalies are evidence of this strong nonlinearity (Figs. 13b, 14b; as identified in Takahashi and Dewitte 2016), as is the large positive skewness in central Pacific wind stress anomalies (Fig. 14d) and in eastern Pacific SST anomalies (Fig. 15d). In contrast, the low-variance epochs are characterized by weaker ENSO events with more linear behavior (Fig. 13a, b; panel c of Fig. 14). From these results we conclude that (1) the physics of the coupled ocean–atmosphere system in CM2.1 are close to linear for the weaker ENSO epochs, resembling the past 50 years; and (2) CM2.1’s high-variance ENSO epochs (such as Epoch H; Fig. 1d) are generated by a collection of stochastically-driven extreme ENSO events that are highly nonlinear. From these analyses we conclude that transient nonlinearities or multiplicative noise help drive the low-frequency ENSO modulation in CM2.1. This is consistent with previous results showing that CM2.1’s ENSO modulation is decadal unpredictable (Wittenberg et al. 2014) and produces rectified effects on the decadal mean state (Ogata et al. 2013).

6 Conclusions

Large, unforced, multi-decadal changes in ENSO variability have been previously reported from the long pre-industrial control run of GFDL CM2.1. We evaluated the possible sources of this low-frequency ENSO modulation, by characterizing the extreme ENSO epochs in CM2.1 and

employing a linearized intermediate-complexity model of the tropical Pacific (LOAM).

Simulations with the linear model demonstrate that intrinsically-generated tropical Pacific decadal mean state changes produced through a rectified nonlinear response to the low frequency ENSO modulation do not contribute to the extreme-ENSO epochs in CM2.1. Rather, these decadal mean state changes actually serve to *damp* the ENSO modulation, primarily by stabilizing the ENSO mode during strong-ENSO epochs. These results point to a possible feedback loop between ENSO and the mean state—whereby noise and nonlinearities produce extreme ENSO epochs, which are then counteracted by linear feedbacks from the mean state. However, it is also possible that in CM2.1, nonlinearities and/or state-dependent noise forcing give rise to mean state feedbacks that are not predicted by the linear model.

The presence of low frequency changes in stochastic (weather) processes is difficult to address using the suite of tools employed in this analysis and thus its contribution to the low-frequency ENSO modulation in CM2.1 has yet to be evaluated. However, we demonstrate (using the linear model runs, CM2.1, and observations) that the low-frequency ENSO modulation can be well described by the simplest model of a linear, stationary process. These results indicate that even in the highly nonlinear CM2.1, ENSO statistics are roughly stationary at multi-decadal time scales (in the absence of external forcings); and the intrinsic low-frequency ENSO modulation in CM2.1 is driven by transient processes operating at interannual or shorter time scales. One might expect nonlinearities, multiplicative noise, and other physics not included in the simple linear model to contribute significantly to the spectral broadening of ENSO, in both the observations and CM2.1. However, we show that their effects on the level of ENSO modulation appear to be weak, compared to the effects of the strong ENSO variance in CM2.1.

We demonstrate that nonlinearities are inextricably linked to the multi-decadal ENSO modulation in CM2.1. High-variance ENSO epochs in CM2.1 are populated by extreme ENSO events that are characterized by a highly nonlinear Bjerknes feedback in the central Pacific; low-variance epochs are characterized by weaker ENSO events with more linear behavior. While nonlinearities in CM2.1 do not dramatically broaden the distribution of variance compared to a linear system with equal long-term ENSO variance, the nonlinearities likely shape the amplitude distribution of ENSO modulation by contributing to an overactive ENSO (e.g. by intensifying strong El Niño events), which then broadens the distribution of epochal ENSO variance.

These results have important implications for understanding the past, present, and future of ENSO. Taken at

face value, CM2.1's strong unforced decadal-to-centennial modulation of ENSO would suggest that existing observational records might be too short to rule out such modulation in the real world (e.g. a factor of four spread in the variance of Niño 3 SSTAs across 40-year epochs). Therefore, to detect a forced change in ENSO variability, e.g. using proxy recorders like Pacific corals to characterize the pre-instrumental epoch, either the records would have to be long or the change large. However, our results suggest that if the past 50 years of observations are representative of the average interannual variance of ENSO in the real world, then the true spectrum of unforced ENSO modulation is, in absolute terms, likely substantially narrower than that suggested by CM2.1. Forced changes might therefore be detectable using relatively short records. However, when relative, rather than absolute, changes in ENSO variance are compared, the distributions of variance are remarkably insensitive to the differing ENSO characteristics. The statistics of the relative changes in ENSO variance might therefore be extrapolated from the fully nonlinear CM2.1 to other systems (e.g. those with less variable and/or more linear ENSOs).

Lastly, we note that tropical Pacific mean state changes due to future greenhouse gas increases are projected to grow substantially larger than the unforced mean state changes seen between the weak-ENSO versus strong-ENSO epochs in CM2.1 (Wittenberg 2015; Xie et al. 2010). Given projected future climate changes in the tropical Pacific, the LOAM-inferred ENSO sensitivity would suggest substantial and detectable changes in ENSO that are consistent with actual forced CM2.1 scenarios (Wittenberg 2015). On the other hand, the LOAM-inferred ENSO sensitivity would also suggest that the mean state biases prevalent in GCMs could have large impacts on how ENSO responds to forcings—underscoring the critical need to reduce these biases, in order to make reliable projections of the future of ENSO.

Acknowledgements This material is based upon work supported by the National Science Foundation Graduate Research Fellowship Program, the Department of Energy Global Change Education Program and the National Oceanic and Atmospheric Administration Climate and Global Change Postdoctoral Program under fellowships to A. Atwood. Support was provided to D. S. Battisti by the Tamaki Foundation. We thank C. Thompson and J. Leloup for their LOAM code and T. Russon for useful discussions that improved this manuscript.

References

- An S-I, Wang B (2000) Interdecadal change of the structure of the ENSO mode and its impact on the ENSO frequency. *J Clim* 13:2044–2055

- Battisti DS (1988) Dynamics and thermodynamics of a warming event in a coupled tropical atmosphere–ocean model. *J Atmos Sci* 45:2889–2919
- Battisti DS, Hirst AC (1989) Interannual variability in a tropical atmosphere ocean model—influence of the basic state, ocean geometry and nonlinearity. *J Atmos Sci* 46:1687–1712
- Bellenger H, Guilyardi E, Leloup J, Lengaigne M, Vialard J (2014) ENSO representation in climate models: from CMIP3 to CMIP5. *Clim Dyn* 42:1999–2018
- Cai WJ, Borlace S, Lengaigne M, van Rensch P, Collins M, Vecchi G, Timmermann A, Santoso A, McPhaden MJ, Wu LX, England MH, Wang GJ, Guilyardi E, Jin FF (2014) Increasing frequency of extreme El Niño events due to greenhouse warming. *Nat Clim Change* 4:111–116
- Capotondi A, Ham Y-G, Wittenberg AT, Kug J-S, (2015) Climate model biases and El Niño Southern Oscillation (ENSO) simulation. *U.S. CLIVAR Variations* 13: 21–25
- Carton JA, Giese BS (2008) A reanalysis of ocean climate using Simple Ocean Data Assimilation (SODA). *Mon Weather Rev* 136:2999–3017
- Chen C, Cane MA, Wittenberg AT, Chen D (2016) ENSO in the CMIP5 simulations: lifecycles, diversity, and responses to climate change. *J Clim* (**in press**)
- Choi KY, Vecchi GA, Wittenberg AT (2013) ENSO transition, duration, and amplitude asymmetries: role of the nonlinear wind stress coupling in a conceptual model. *J Clim* 26:9462–9476
- Choi KY, Vecchi GA, Wittenberg AT (2015) Nonlinear zonal wind response to ENSO in the CMIP5 models: roles of the zonal and meridional shift of the ITCZ/SPCZ and the simulated climatological precipitation. *J Clim* 28:8556–8573
- Cobb KM, Westphal N, Sayani HR, Watson JT, Di Lorenzo E, Cheng H, Edwards RL, Charles CD (2013) Highly variable El Niño–Southern Oscillation throughout the holocene. *Science* 339:67–70
- Collins M, An SI, Cai WJ, Ganachaud A, Guilyardi E, Jin FF, Jochum M, Lengaigne M, Power S, Timmermann A, Vecchi G, Wittenberg A, (2010) The impact of global warming on the tropical Pacific ocean and El Niño. *Nat Geosci* 3:391–397
- Delworth TL, Broccoli AJ, Rosati A, Stouffer RJ, Balaji V, Beesley JA, Cooke WF, Dixon KW, Dunne J, Dunne KA, Durachta JW, Findell KL, Ginoux P, Gnanadesikan A, Gordon CT, Griffies SM, Gudgel R, Harrison MJ, Held IM, Hemler RS, Horowitz LW, Klein SA, Knutson TR, Kushner PJ, Langenhorst AR, Lee HC, Lin SJ, Lu J, Malyshev SL, Milly PCD, Ramaswamy V, Russell J, Schwarzkopf MD, Shevliakova E, Sirutis JJ, Spelman MJ, Stern WF, Winton M, Wittenberg AT, Wyman B, Zeng F, Zhang R (2006) GFDL’s CM2 global coupled climate models. Part I: Formulation and simulation characteristics. *J Clim* 19:643–674
- Dewitte R (2000) Sensitivity of an intermediate ocean–atmosphere coupled model of the tropical Pacific to its oceanic vertical structure. *J Clim* 13:2363–2388
- DiNezio PN, Kirtman BP, Clement AC, Lee SK, Vecchi GA, Wittenberg A (2012) Mean climate controls on the simulated response of ENSO to increasing greenhouse gases. *J Clim* 25:7399–7420
- Gill AE (1980) Some simple solutions for heat-induced tropical circulation. *Q J R Meteorol Soc* 106:447–462
- Graham FS, Wittenberg AT, Brown JN, Marsland SJ, Holbrook NJ (2016) Understanding the double peaked El Niño in coupled GCMs. *Clim Dyn* (**in press**)
- Guilyardi E, Wittenberg A, Fedorov A, Collins M, Wang C, Capotondi A, van Oldenborgh J, Stockdale T (2009) Understanding El Niño in ocean–atmosphere general circulation models. *Bull Am Meteorol Soc* 90:325–340
- Guilyardi E, Bellenger H, Collins M, Ferrett S, Cai W, Wittenberg A (2012a) A first look at ENSO in CMIP5. *Clivar Exch* 58:29–32
- Guilyardi E, Cai WJ, Collins M, Fedorov A, Jin FF, Kumar A, Sun DZ, Wittenberg A (2012b) New strategies for evaluating ENSO processes in climate models. *Bull Am Meteorol Soc* 93:235–238
- Guilyardi E, Wittenberg A, Balmaseda M, Cai W, Collins M, McPhaden M, Watanabe M, Yeh S-W (2016) ENSO in a changing climate: meeting summary of the 4th CLIVAR workshop on the evaluation of ENSO processes in climate models. *Bull Am Meteorol Soc* (**in press**)
- Ham YG, Kug JS, Kim D, Kim YH, Kim DH (2013) What controls phase-locking of ENSO to boreal winter in coupled GCMs? *Clim Dyn* 40:1551–1568
- Karamperidou C, Cane MA, Lall U, Wittenberg AT (2014) Intrinsic modulation of ENSO predictability viewed through a local Lyapunov lens. *Clim Dyn* 42:253–270
- Koutavas A, Demenocal PB, Olive GC, Lynch-Stieglitz J (2006) Mid-Holocene El Niño–Southern Oscillation (ENSO) attenuation revealed by individual foraminifera in eastern tropical Pacific sediments. *Geology* 34:993–996
- Kug JS, Choi J, An SI, Jin FF, Wittenberg AT (2010) Warm pool and cold tongue El Niño events as simulated by the GFDL 2.1 coupled GCM. *J Clim* 23:1226–1239
- Levine AFZ, Jin FF (2016) A simple approach to quantifying the noise-ENSO interaction. Part 1: deducing the state-dependency of the windstress forcing using monthly mean data. *Clim Dyn* (**in press**)
- McGregor HV, Fischer MJ, Gagan MK, Fink D, Phipps SJ, Wong H, Woodroffe CD (2013) A weak El Niño/Southern Oscillation with delayed seasonal growth around 4,300 years ago. *Nat Geosci* 6:949–953
- Newman M, Alexander MA, Scott JD (2011) An empirical model of tropical ocean dynamics. *Clim Dyn* 37:1823–1841
- Ogata T, Xie SP, Wittenberg A, Sun DZ (2013) Interdecadal amplitude modulation of El Niño–Southern Oscillation and its impact on tropical Pacific decadal variability. *J Clim* 26:7280–7297
- Penland C, Sardeshmukh PD (1995) The optimal growth of tropical sea surface temperature anomalies. *J Clim* 8:1999–2024
- Reichler T, Kim J (2008) Uncertainties in the climate mean state of global observations, reanalyses, and the GFDL climate model. *J Geophys Res* 113:D05106
- Roberts W (2007) An investigation into the causes for the reduction in the variability of the El Niño–Southern Oscillation in the early holocene in a global climate model. University of Washington, Seattle, p 145
- Roberts WHG, Battisti DS (2011) A new tool for evaluating the physics of coupled atmosphere–ocean variability in nature and in general circulation models. *Clim Dyn* 36:907–923
- Roberts WHG, Battisti DS, Tudhope AW (2014) ENSO in the Mid-Holocene according to CSM and HadCM3. *J Clim* 27:1223–1242
- Russon T, Tudhope AW, Hegerl GC, Schurer A, Collins M (2014) Assessing the significance of changes in ENSO amplitude using variance metrics. *J Clim* 27:4911–4922
- Takahashi K, Dewitte B (2016) Strong and moderate nonlinear El Niño regimes. *Clim Dyn* 46:1627–1645
- Taschetto AS, Sen Gupta A, Jourdain NC, Santoso A, Ummerhofer CC, England MH (2014) Cold tongue and warm pool ENSO events in CMIP5: mean state and future projections. *J Clim* 27:2861–2885
- Thompson CJ (1998a) Initial conditions for optimal growth in a coupled ocean–atmosphere model of ENSO. *J Atmos Sci* 55:537–557
- Thompson CJ (1998b) A linear, stochastic, dynamical model of El Niño /Southern Oscillation. University of Washington, Seattle
- Thompson CJ, Battisti DS (2000) A linear stochastic dynamical model of ENSO. Part I: model development. *J Clim* 13:2818–2832

- Thompson CJ, Battisti DS (2001) A linear stochastic dynamical model of ENSO. Part II: analysis. *J Clim* 14:445–466
- Timmermann A, Jin FF (2002) A nonlinear mechanism for decadal El Niño amplitude changes. *Geophys Res Lett* 29:1003
- Tudhope AW, Chilcott CP, McCulloch MT, Cook ER, Chappell J, Ellam RM, Lea DW, Lough JM, Shimmield GB (2001) Variability in the El Niño-Southern oscillation through a glacial-interglacial cycle. *Science* 291:1511–1517
- van Oldenborgh GJ, Philip SY, Collins M (2005) El Niño in a changing climate: a multi-model study. *Ocean Sci* 1:81–95
- Vecchi GA, Wittenberg AT, Rosati A (2006) Reassessing the role of stochastic forcing in the 1997–1998 El Niño. *Geophys Res Lett* 33:L01706
- Vimont DJ (2005) The contribution of the interannual ENSO cycle to the spatial pattern of decadal ENSO-like variability. *J Clim* 18:2080–2092
- von Storch H, Zwiers FW (2003) *Statistical analysis in climate research*. Cambridge University Press, 484 pp
- Watanabe M, Kug JS, Jin FF, Collins M, Ohba M, Wittenberg AT (2012) Uncertainty in the ENSO amplitude change from the past to the future. *Geophys Res Lett* 39:L20703
- Wittenberg A (2002) *ENSO response to altered climates*. Princeton University, Princeton, p 475
- Wittenberg AT (2009) Are historical records sufficient to constrain ENSO simulations? *Geophys Res Lett* 36:L12702
- Wittenberg A (2015) Low-frequency variations of ENSO. *U.S. CLIVAR Variations* 13:26–31
- Wittenberg AT, Rosati A, Lau NC, Ploshay JJ (2006) GFDL's CM2 global coupled climate models. Part III: tropical pacific climate and ENSO. *J Clim* 19:698–722
- Wittenberg AT, Rosati A, Delworth TL, Vecchi GA, Zeng FR (2014) ENSO modulation: is it decadal predictability? *J Clim* 27:2667–2681
- Xie SP, Deser C, Vecchi GA, Ma J, Teng HY, Wittenberg AT (2010) Global warming pattern formation: sea surface temperature and rainfall. *J Clim* 23:966–986
- Zebiak SE, Cane MA (1987) A model El Niño-Southern Oscillation. *Mon Weather Rev* 115:2262–2278